JOURNAL OF MATERIALS SCIENCE **35** (2000) 3693–3697

R-curve behaviour and microstructure of liquid-phase sintered α-SiC

JAE-YEON KIM, HYUN-GU AN, YOUNG-WOOK KIM*
Department of Materials Science and Engineering, The University of Seoul, Seoul 130-743, Korea
E-mail: ywkim@uoscc.uos.ac.kr

M. MITOMO
National Institute for Research in Inorganic Materials, Ibaraki 305, Japan

R-curves for two liquid-phase sintered α-SiC (SC-A and SC-B), of different microstructures, were characterized using indentation-strength method. Silicon carbide SC-B, with its coarser microstructure and 8 MPa $\cdot$ m$^{1/2}$ toughness, showed higher resistance to crack growth and more damage tolerance than silicon carbide SC-A, with its finer microstructure and 4.5 MPa $\cdot$ m$^{1/2}$ toughness. These results suggest that a coarse microstructure is beneficial to toughening and damage tolerance while a fine microstructure is beneficial to strengthening.

1. Introduction

Many ceramics demonstrate increasing fracture toughness with increasing crack length [1–9]. This *R*-curve behavior arises because of the interactions of the microstructure behind the crack tip in the wake region. Specifically, on nontransforming systems such as alumina [2, 3], silicon nitride [4–6], and *in-situ* toughened silicon carbide [7–9], the *R*-curve derives from the development of a zone of bridging grains behind the crack tip, which reduces the near-tip driving force and retards subsequent crack extension.

It has been demonstrated that the shape of the *R*-curve influences strength variability and damage tolerance and the fracture toughness of silicon carbide is dependent on its microstructure [10–12]. Also, a tradeoff in improving both the strength and toughness has been reported in SiC ceramics with self-reinforced microstructure [13]. Therefore, an understanding of the relation between *R*-curve behavior and microstructure of SiC is important to achieve tough and reliable materials.

Padture and Lawn [7] demonstrated that a heterogeneous SiC with a coarsened and elongated microstructure and an intergranular second phase exhibits an enhanced toughness in the long-crack region and a degraded toughness in the short crack region, relative to a homogeneous, fine-grained SiC (Hexoloy SA, Carborundum, Niagara Falls, NY, U.S.A.). Gilbert *et al.* [9] investigated the *R*-curve behavior of two SiC ceramics (an *in situ*-toughened SiC doped with Al, B and C as sintering aids and an Hexoloy SA). The *in situ*-toughened SiC exhibited much-improved flaw tolerance with significant rising *R*-curve behavior and a steady-state fracture toughness of $\sim$9 MPa $\cdot$ m$^{1/2}$ after crack extension of $\sim$600 μm while Hexoloy SA showed a flat *R*-curve. An investigation of the effect of microstructure on *R*-curve, keeping sintering aid (i.e., grain boundary composition) constant, showed that an *in situ*-toughened microstructure, consisted of mostly 4H polytype, exhibited more sharply rising *R*-curve behavior than an equiaxed microstructure [8].

Recently, a new self-reinforced microstructure, consisted of mostly 6H, has been developed from α-SiC starting powders [14, 15]. The self-reinforced microstructure can be obtained from α-starting powder by (1) controlling the initial particle size distribution, (2) adding a small amount of oxides as sintering aids, and (3) sintering or annealing at high temperatures ($\geq$1900°C) [14]. The SiC had a short-crack fracture toughness of $\sim$5.5 MPa $\cdot$ m$^{1/2}$. This improved fracture toughness was attributed to crack bridging and deflection by elongated grains. As a result of these toughening mechanisms, this liquid-phase-sintered α-SiC would be expected to have rising *R*-curve behavior and excellent flaw tolerance.

In the present study, the *R*-curve behaviour for two liquid-phase sintered α-silicon carbides A and B, consisted of mostly polytype 6H, of different microstructures was investigated using the indentation-strength method. The silicon carbide A was a hot-pressed and subsequently annealed α-SiC, fabricated from α-SiC powder without seeds, with relatively fine, equiaxed microstructure and an unimodal grain size distribution. The silicon carbide B was also a hot-pressed and subsequently annealed α-SiC, fabricated from α-SiC powder containing large α-SiC seeds, with relatively coarse, self-reinforced microstructure and a bimodal grain size distribution. The SiC-A has a higher strength while SiC-B has a higher toughness. Microstructure analysis,

* Author to whom all correspondence should be addressed.

indentation load-strength analysis (strength measured as a function of indentation load), and a crack-wake observation were used to correlate the *R*-curve with the microstructure.

2. Experimental procedure

Commercially available fine α-SiC powder (A-1 grade, Showa Denko, Tokyo, Japan; designated as F) and relatively coarse α-SiC powder (UF-10 grade, Lonza-Werke Gmbh, Wald-shut-Tiengen, Germany; designated as L) were used as starting powders. Powder L was added as seeds for grain growth. To prepare a powder composition without seeds, 88 wt% powder F, 8.8 wt% $Y_3Al_5O_{12}$ (yttrium-aluminum garnet, YAG, High Purity Chemicals, 99.99% pure, Osaka, Japan) and 3.2 wt% SiO_2 (Kanto Chemical Co., Inc., reagent grade, Tokyo, Japan) were ball milled in ethanol with SiC grinding balls for 24 h. To prepare a powder composition containing seeds, 85 wt% powder F, 8.8 wt% $Y_3Al_5O_{12}$ and 3.2 wt% SiO_2 were ball milled in ethanol for 20 h, then 3 wt% powder L was added, followed by additional milling for 4 h. The milled slurry was dried and hot-pressed at 1820°C for 1 h under a pressure of 25 MPa in argon atmosphere. The hot-pressed specimens without seeds were further annealed at 1920°C for 2 h without pressure under an atmospheric pressure of Ar to enhance grain growth. The 2-h -annealed material was designated as SC-A. The hot-pressed specimens containing seeds were further annealed at 1920°C for 8 h without pressure under an atmospheric pressure of Ar to enhance grain growth. The 8-h-annealed material was designated as SC-B.

The bulk densities of the sintered samples were determined by the Archimedes method. The theoretical density of the samples, 3.260 $g \cdot cm^{-3}$, was calculated according to the rule of mixtures. The hot-pressed and annealed materials were cut and polished, then etched with a plasma of CF_4 containing 7.8% O_2. The microstructures were observed by scanning electron microscopy (SEM). The microstructures of the annealed materials have been quantitatively analyzed using image analysis (Image-Pro Plus, Media Cybernetics, Maryland, USA) according to a procedure shown in previous studies [13, 16]. X-ray diffraction (XRD) using Cu K_α radiation was performed on the ground powders.

Specimens for *R*-curve test were cut and polished into 3 mm × 2.5 mm × 25 mm bars up to 1 μm finish. Prior to indentation, a thin film of gold was deposited on the indentation surface for accurate observation of the crack size and a drop of moisture-free silicon oil was spread over the site of the indentation for minimizing moisture-assisted subcritical crack growth of as-indented cracks. Special care was taken to orient the radial cracks generated from the indentation parallel to the sides of the bar. Three Vickers indentations with loads ranging from 1.96 to 294 N were made 3 mm apart in the centre of the prospective tensile surface of each test piece. A total of 32 indented bars for each of SC-A and SC-B were directly fractured using four point bending. Every specimen was checked to ensure that fracture was initiated from the indent. The average strength data obtained from the four specimens that fractured from the indented sites were used for the subsequent *R*-curve analysis as described by Krause [17].

3. Results and discussion

3.1. Microstructure

The characteristics of annealed α-SiC are summarized in Table I. The relative densities of SC-A and B materials were 98.2% and 98.4%, respectively. SEM micrographs of polished and etched surfaces are shown in Fig. 1. As shown, SC-A had an unimodal microstructure consisting of relatively fine, equiaxed grains, while SC-B had a duplex microstructure consisting of small matrix grains and large elongated grains.

Phase analysis of the annealed materials by XRD showed that the major phase in each specimen was polytype 6H (Table I). These results show that the growth of platelet-shaped grains resulted mainly from the

TABLE I Characteristics of liquid-phase-sintered α-SiC ceramics used in this study

Material	Relative density (%)	Bending strength (MPa)	Fracture toughness ($MPa \cdot m^{1/2}$)	Crystalline phase	
				Major	Trace
SC-A	98.2	561	4.5	6H	YAG*
SC-B	98.4	490	8.0	6H	4H, YAG

*$Y_3Al_5O_{12}$ (yttrium aluminum garnet).

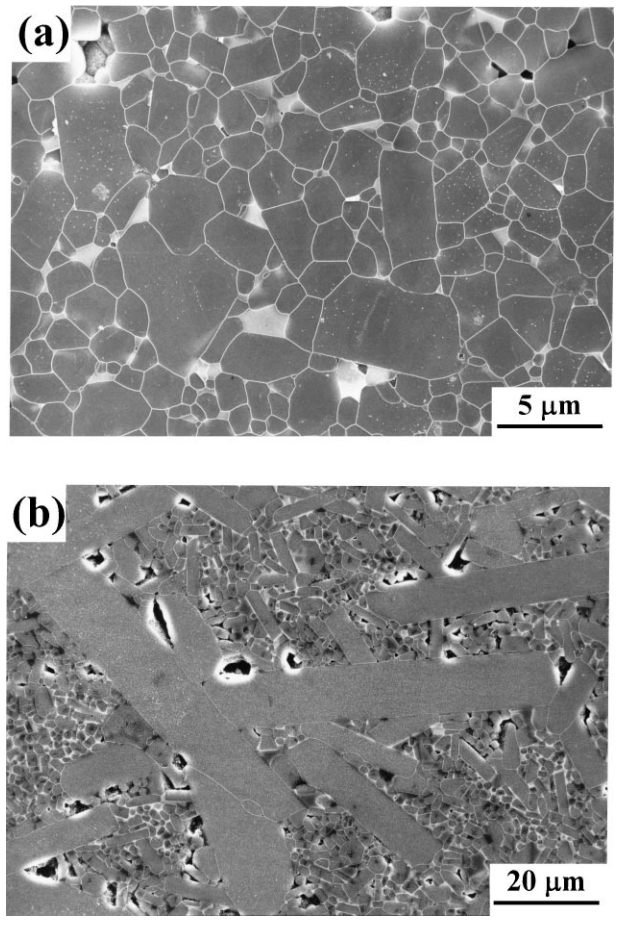

Figure 1 Typical microstructures of polished and etched silicon carbide surfaces: (a) SC-A and (b) SC-B (refer to Table I).

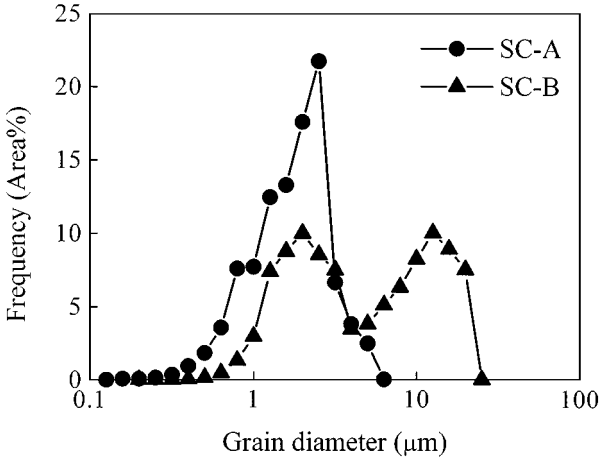

Figure 2 Grain-size distribution revealed by the relation between grain diameter and areal frequency for SC-A and SC-B (refer to Table I).

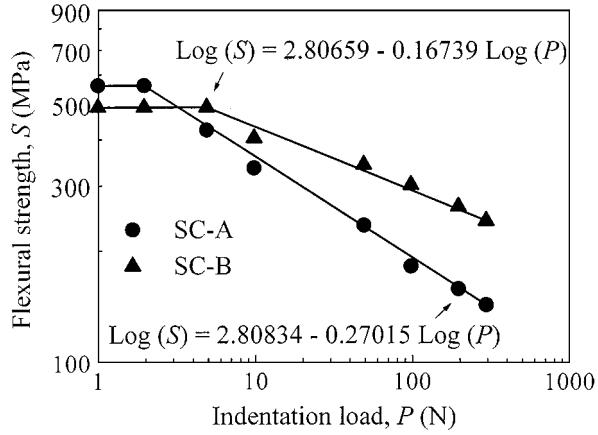

Figure 3 Plots of strength versus indentation load for SC-A and SC-B (refer to Table I). The natural strengths were arbitrarily plotted at $P = 1$ N.

overgrowth of α-SiC on the starting powder (polytype 6H) via solution-precipitation [18]. The self-reinforced material (SC-B) has a similar microstructure with self-reinforced materials (consisted of mostly 4H) prepared from β-SiC powders [19], but a different polytype of SiC. The SC-B material contained YAG and 4H as the secondary phases.

Image analysis of the two annealed specimens was conducted to evaluate the microstructure quantitatively. The grain-diameter distribution and aspect-ratio distribution for each material were obtained. Grain diameter was evaluated as the thickness observed in a two-dimensional cross-section. The frequency distribution was expressed in terms of the percentage of the total area occupied by grains of the same diameter size. An areal percent in a two-dimensional observation approximately corresponds to volume percent in a three-dimensional observation [20]. Fig. 2 shows the grain-diameter distribution for SC-A and SC-B. SC-A had a monomodal grain-diameter distribution ranging from 0.2–6.3 μm. On the other hand, SC-B had a bimodal grain-diameter distribution of an equiaxed matrix grain-diameter distribution ranging from 0.3–4.0 μm and an elongated grain-diameter distribution ranging from 4.0–20 μm. The separation point between the large grains and matrix grains, determined from the grain-diameter distribution, was 4.0 μm for SC-B material. The mean aspect ratio of elongated grains for SC-B material was 5.6. This value is slightly higher than that ($\sim$4) of "*in situ*-toughened microstructure," fabricated from β-SiC starting powders [13, 16].

3.2. *R*-curve behavior

The fracture strength versus indentation load for SC-A and SC-B materials is shown in Fig. 3. The natural strengths of both specimens were arbitrarily plotted at $P = 1$ N. Every specimen was checked to ensure that fracture was initiated from the indent. Bending strength for SC-A reached to its natural strength at 1.96 N indentation. However, bending strength for SC-B reached to its natural strength at 4.9 N indentation. This result suggests that SC-B, which has a coarser, duplex microstructure, is a more damage tolerant material than SC-A. It is also supported by the crossover of strength, which takes place between 1.96 and 4.9 N. Initially SC-A has about 14% higher strength than SC-B. However, after 4.9 N indentation, SC-A loses about 24% of its initial strength, while SC-B has its natural strength and becomes a stronger material than SC-A. Extremely large elongated grains or clusters of large grains in silicon carbide with a duplex microstructure are believed to act as a fracture origin [14]. As shown in Fig. 1, the microstructure of SC-B has a duplex microstructure consisted of large elongated grains and relatively fine matrix grains, while the microstructure of SC-A without seeds consisted of fine, equiaxed α-SiC grains. Considering the microstructural features, the critical flaw size of SC-B may be larger than that of SC-A. The improved flaw tolerance of SC-B can be attributed to the presence of large, elongated grains as shown in Fig. 1b. Hence, it is reasonable that SC-B is more damage tolerant than SC-A. The above results also suggest that SC-B may have a higher fracture resistance than SC-A.

Linear regression was used to obtain the best fit lines for the data from SC-A and SC-B. It showed that slopes of SC-A and SC-B were 0.27015 and 0.16739, respectively. Griffith materials, which show no rising *R*-curve behavior, have a slope of 1/3, and *R*-curve materials have lower slopes [17]. Because of the slopes of both materials are less than 1/3, rising *R*-curve behavior is expected for both materials.

R-curve behaviour was estimated from the indentation strength data in Fig. 3 by assuming that the fracture resistance (K_R) is related to the crack length (c) by a power-law relation, as suggested by Krause [17]. The power-law relation is a strictly empirical relation, and is used simply as a means to obtain estimates of the *R*-curve. Table II summarizes the important parameters

TABLE II Important parameters* defining fracture resistance

	β	$\log \alpha$	$\log \gamma$	Y	m	k
SC-A	0.27015	2.81	8.32	1.174	0.091	8.7
SC-B	0.16739	2.81	8.92	1.174	0.213	37.1

*Refer to Reference [17].

needed for estimation of the R-curve for SC-A and SC-B. The estimated R-curves for SC-A and SC-B are shown in Fig. 4, where the predicted fracture resistance curves as a function of crack size are given. As shown, both materials have rising crack-growth resistance behavior, i.e., R-curves with toughening exponents of $m = 0.091$ and 0.213 for SC-A and SC-B, respectively. m is a constant reflecting the extent of R-curve behavior for the material. SC-B has higher values of K_R than SC-A in the measured crack size range between 31 to 941 μm, as expected from the indentation-results (Fig. 3).

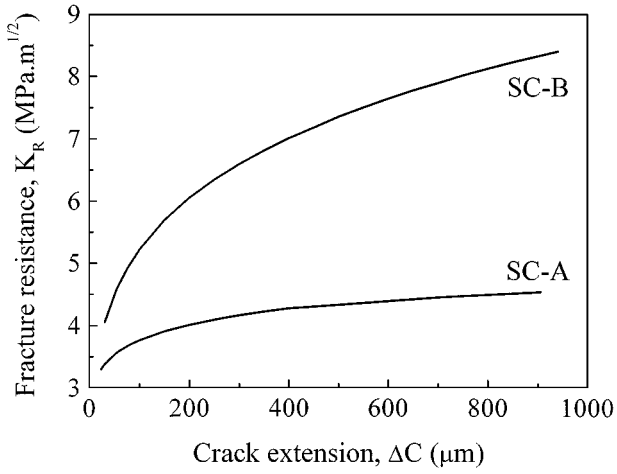

Figure 4 Rising crack-growth resistance curves (R-curve) as a function of crack size for SC-A and SC-B (refer to Table I).

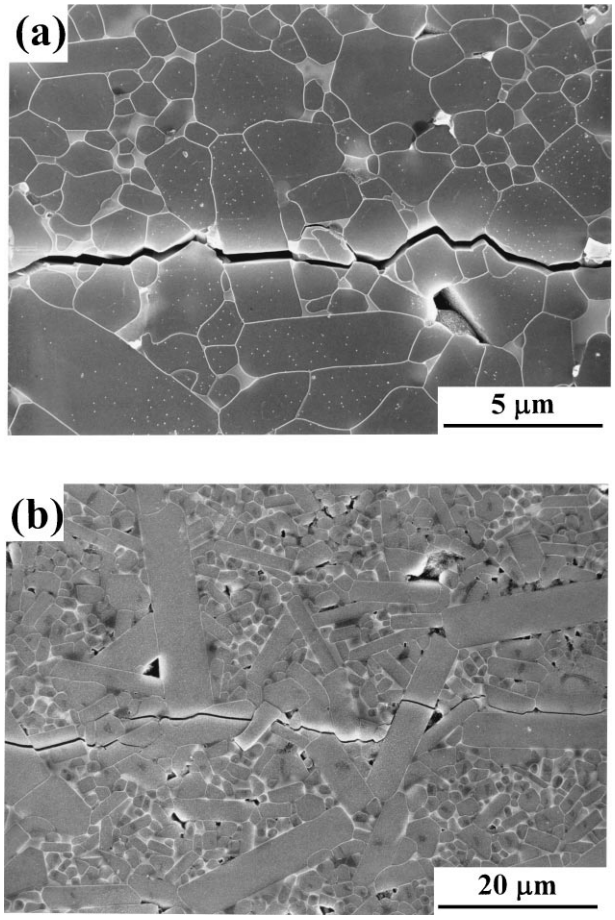

Figure 5 SEM micrographs of crack paths induced by a Vickers indentation in (a) SC-A and (b) SC-B (refer to Table I).

In silicon carbide ceramics with duplex microstructure, a principal source of increased fracture toughness is believed to be grain bridging by elongated grains and/or matrix grains behind the crack tip [15, 19]. As the fracture front advances, the grain bridging sites are left behind and provide a restraining force which must ultimately be overcome for failure to occur. SEM micrographs indicate some evidence of bridging grains in SiC ceramics (Fig. 5b). As shown in Fig. 5, the crack trajectories in SC-A and SC-B were mostly localized in the glass phase and mostly around the SiC grains. The crack bridging was more pronounced in SC-B. We note that at each bridge-rupture site, the cumulative amount of surface-exposed crack length is approximately two to three times the shortest straight-line path through the bridging sites. Moreover, the fracture surface area incorporates an amount of transgranular fracture near the bridging grain. Because the grain boundary is weaker than the matrix single crystal (for otherwise most of the fracture would be transgranular), transgranular fracture needs higher energy than intergranular fracture. Therefore, bridges clearly represent an high-energy source of fracture resistance. It is recognized here, of course, that contributions of other toughening mechanisms, for example, crack deflection, cannot be ruled out [21].

4. Conclusions

R-curve behavior for two silicon carbides, consisted of mostly polytype 6H, with different microstructures were determined by the indentation-strength method. The flaw tolerance and R-curve behaviour depended highly on the microstructural features. Liquid-phase-sintered SC-A and SC-B exhibited rising R-curve behaviour with toughening exponents of $m = 0.091$ and $m = 0.213$, respectively. SC-B consisted of large, elongated grains and fine, equiaxed matrix grains, exhibited better flaw tolerance and more sharply rising R-curve behaviour than the SC-A consisted of relatively fine, equiaxed grains.

Acknowledgement

This work was supported by Korean Research Foundation under Grant No. KRF-99-042-E00133.

References

1. P. BECHER, *J. Amer. Ceram. Soc.* **74** (1991) 255.
2. R. KNEHANS and R. W. STEINBRECH, *J. Mater. Sci. Lett.* **1** (1982) 327.
3. P. L. SWANSON, C. J. FAIRBANKS, B. R. LAWN, Y.-W. MAI and B. J. HOCKEY, *J. Amer. Ceram. Soc.* **70** (1987) 279.
4. C. W. LI and J. YAMANIS, *Ceram. Eng. Sci. Proc.* **10** (1989) 632.
5. S. R. CHOI, J. A. SALEM and W. A. SANDERS, *J. Amer. Ceram. Soc.* **75** (1992) 1508.
6. Y.-W. KIM, M. MITOMO and N. HIROSAKI, *J. Mater. Sci.* **30** (1995) 4043.
7. N. P. PADTURE and B. R. LAWN, *J. Amer. Ceram. Soc.* **77** (1994) 2518.
8. S. K. LEE, D. K. KIM and C. H. KIM, *ibid.* **78** (1995) 65.

9. C. J. GILBERT, J. J. CAO, L. C. DEJONGHE and R. O. RITCHIE, *ibid.* **80** (1997) 2253.
10. R. F. COOK and D. R. CLARKE, *Acta Metall.* **36** (1988) 555.
11. D. K. SHETTY and J. S. WANG, *J. Amer. Ceram. Soc.* **72** (1989) 1158.
12. S. J. BENNISON and B. R. LAWN, *J. Mater. Sci.* **24** (1989) 3169.
13. Y.-W. KIM, M. MITOMO, H. EMOTO and J. G. LEE, *J. Amer. Ceram. Soc.* **81** (1998) 3136.
14. J. Y. KIM, Y.-W. KIM, J. G. LEE and K. S. CHO, *J. Mater. Sci.* **34** (1999) 2325.
15. J. Y. KIM, Y.-W. KIM, M. MITOMO, G. D. ZHAN and J. G. LEE, *J. Amer. Ceram. Soc.* **82** (1999) 441.
16. Y.-W. KIM, M. MITOMO and H. HIROTSURU, *ibid.* **80** (1997) 99.
17. R. F. KRAUSE, *ibid.* **71** (1988) 338.
18. L. S. SIGL and H. J. KLEEBE, *ibid.* **76** (1993) 773.
19. N. P. PADTURE, *ibid.* **77** (1994) 519.
20. N. HIROSAKI, Y. AKIMUNE and M. MITOMO, *J. Ceram. Soc. Jpn.* **101** (1993) 1239.
21. M. A. MULLA and V. D. KRSTIC, *Acta Metall. Mater.* **77** (1994) 303.

Received 4 January
and accepted 24 January 2000